

# On the Gas Phase Hydrogen Bond Complexes between Formic Acid and Hydroperoxyl Radical. A Theoretical Study

M. Torrent-Sucarrat<sup>†</sup> and J. M. Anglada<sup>\*‡</sup>

*Institut de Química Computacional and Departament de Química, Universitat de Girona, E-17071 Girona, Catalonia, Spain, and Departament de Química Orgànica Biològica, Institut d'Investigacions Químiques i Ambientals de Barcelona, I.I.Q.A.B.–C.S.I.C., c/Jordi Girona 18, E-08034 Barcelona, Catalonia, Spain*

*Received: February 10, 2006; In Final Form: May 30, 2006*

We present a systematic study on the gas-phase hydrogen-bonded complexes formed between formic acid and hydroperoxyl radical, which has been carried out by using B3LYP and CCSD(T) theoretical approaches in connection with the 6-311+G(2df,2p) basis set. For all complexes we have employed the AIM theory by Bader and the NBO partition scheme by Weinhold to analyze the bonding features. We have found 17 stationary points, and 11 of them present a cyclic structure. Their computed stabilities vary from 0.3 to 11.3 kcal/mol, depending on several factors, such as involvement in the hydrogen bond interaction, the geometrical constraints, and the possible concurrence of further effects such as resonance-assisted hydrogen bonds or inductive effects. In addition, three stationary points correspond to transition structures involving a double proton-transfer process whose features are also analyzed.

## I. Introduction

Hydrogen bonding is the most relevant noncovalent intermolecular interaction and it governs many chemical and biological processes in nature.<sup>1–3</sup> Due to this importance, many theoretical and experimental studies have been done to characterize the nature of the hydrogen bond. Despite of the large amount of research work devoted to this issue, the study of hydrogen-bonded complexes is still an open question.<sup>4–8</sup>

Most of the investigations carried out refer to hydrogen-bonded complexes formed between neutral molecules or between a neutral molecule and an ion. However, in the recent years an increased interest has been observed in the study of radical–molecule hydrogen-bonded complexes, because of their importance in the chemistry of the atmosphere<sup>9–27</sup> and in biological<sup>28–30</sup> systems as well. Thus, regarding the study of the gas-phase radical–molecule hydrogen-bonded complexes, it has been proven that they have an important role in the kinetic behavior of many atmospheric reactions, but additionally, they can contribute to the spread of contamination through the atmosphere or to formation of aerosols.<sup>10,21</sup>

Recent studies reported in the literature have shown that relative strong hydrogen-bonded complexes are formed in the gas phase between hydroperoxyl radical and different species<sup>9,16–18,27,31</sup> and in the present investigation, we have focused our attention on the gas-phase hydrogen-bonded complexes formed between hydroperoxyl radical (HO<sub>2</sub><sup>\*</sup>) and formic acid (HCOOH), which are two important species in atmospheric chemistry.<sup>32–35</sup> The most stable hydrogen-bonded complex between hydroperoxyl radical and formic acid has been extensively reported in the literature,<sup>11,19,27</sup> and in this work we have extended the study to the investigation of all species that can be formed between both the syn and anti conformers of formic acid with hydroperoxyl radical in the gas phase. This

investigation also includes several processes in which a double hydrogen transfer process (dhtp) occurs between both species and constitutes an extension of previous work on the hydrogen-bonded complexes formed between hydroxyl radical and formic acid recently reported in the literature.<sup>21,25</sup> Due to the fact that both HO<sub>2</sub><sup>\*</sup> and HCOOH have several hydrogen-donor and hydrogen-acceptor sites, this study will provide information regarding the different donor and/or acceptor abilities of the groups of both molecules that are able to form hydrogen bonds and also the features governing the cooperative effects in those complexes being stabilized by more than one hydrogen bond. For this analysis we have employed the atoms in molecules (AIM) theory by Bader<sup>36,37</sup> and the NBO partitioning scheme by Weinhold,<sup>38</sup> which have been proven to be very valuable in the study and characterization of hydrogen bonds and cooperative effects.<sup>5,19,25,39–47</sup>

## II. Computational Details

All calculations performed in this work have been carried out by using the Gaussian98 program package.<sup>48</sup> The geometries for all stationary points have been optimized using the 6-311+G-(2df,2p) basis set<sup>49</sup> employing the unrestricted density functional Becke's three parameter and Lee–Yang–Parr functional (B3LYP) method.<sup>50</sup> At this level of theory, we have also calculated the harmonic frequencies in order to verify the nature of the corresponding stationary points (minima or transition states) and to provide the zero-point vibrational energy (ZPVE) and the thermodynamic contribution to the enthalpy for 298 K. In addition, we have done intrinsic reaction coordinate calculations on the transition states to check the connection with the reactants and products.

With the aim to get more reliable relative energies, single point CCSD(T)<sup>51–53</sup> calculations have been performed at the B3LYP-optimized geometries. Moreover, a better estimation of the energetic stability of the hydrogen-bonded complexes found in this investigation has been obtained using the basis set superposition error (BSSE) computed at the CCSD(T) level of

\* Corresponding author. E-mail: anglada@iiqab.csic.es.

<sup>†</sup> Universitat de Girona.

<sup>‡</sup> Institut d'Investigacions Químiques i Ambientals de Barcelona.

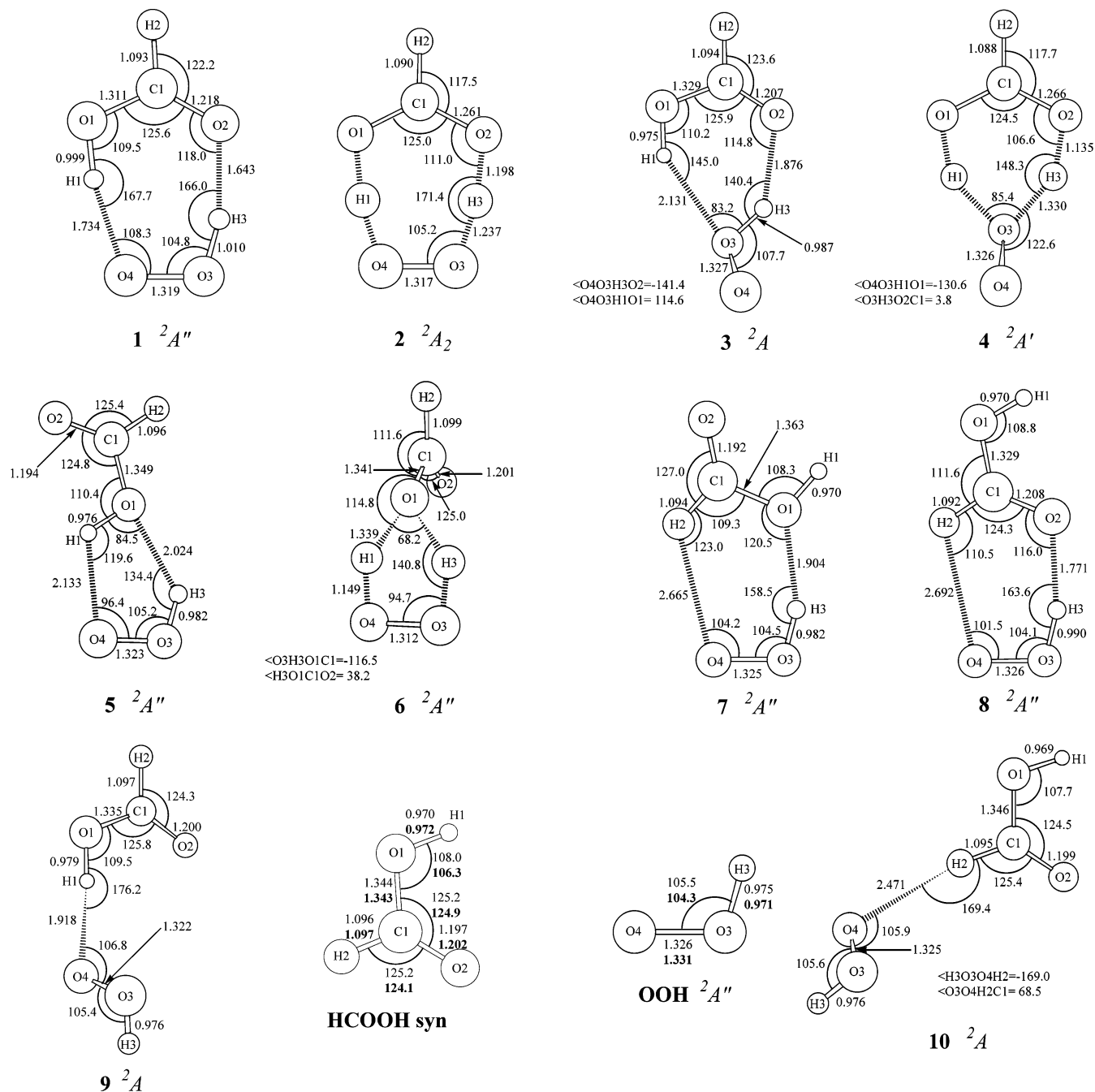


**Figure 1.** Selected geometrical parameters of the B3LYP/6-311+G(2df,2p)-optimized geometries for complexes formed between *syn*-HCOOH and HOO<sup>•</sup>. The distances and angles in bold are the experimental values of the *syn*-HCOOH and HOO<sup>•</sup>. Distances are given in angstroms and angles in degrees.

theory according to the counterpoise method by Boys and Bernardi.<sup>54</sup> Finally, the bonding features of the different complexes investigated have been analyzed according to the atoms in molecules (AIM) theory by Bader, whereas the charge distribution was obtained following the natural bond orbital (NBO) partition scheme by Weinhold and co-workers.<sup>38</sup> The topological properties of wave functions were computed using the AIM-PAC program package.<sup>55</sup>

The Cartesian coordinates of all stationary points and the absolute energies and enthalpies are available as Supporting Information.

### III. Results and Discussion

Formic acid has two hydrogen donors and two hydrogen acceptors, while the hydroperoxyl radical has one hydrogen

donor and two hydrogen acceptors. Consequently, several hydrogen-bonded complexes can be formed between both molecules, and their geometries and stabilities depend on the H-donor and H-acceptor abilities of the groups involved in each electronic interaction. In fact, in this work we have found 10 stationary points (structures 1–10) forming complexes between *syn*-HCOOH and HO<sub>2</sub><sup>•</sup> radical and seven stationary points (structures 11–17) forming complexes between *anti*-HCOOH and HO<sub>2</sub><sup>•</sup> radical.

Figures 1 and 4 display the most relevant geometrical parameters of the hydrogen-bonded complexes formed between *syn/anti*-formic acid molecule and HOO<sup>•</sup> radical, respectively. It is worth noting that the optimized geometrical parameters for HCOOH and HOO<sup>•</sup> agree quantitatively with experimental<sup>56–58</sup> values and theoretical<sup>22,59,60</sup> results from the litera-

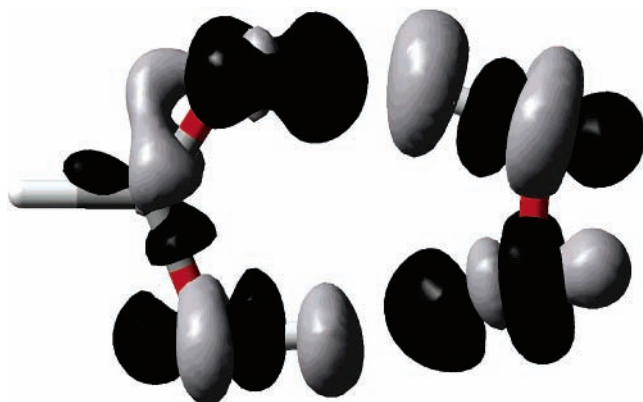


**Figure 2.** Representation of the B3LYP/6-311+G(2df,2p) electron density difference isosurfaces for complex **1**. Black regions correspond to increased electron density caused by the intermolecular interactions and gray regions represent depleted electron density. The contour shown is 0.003.

ture. Figure 2 displays the representation of the electron density difference for the complex **1**. The electron density difference is obtained by subtracting the electronic density of each fragment (HCOOH and HOO<sup>•</sup>) from the total electronic density of the complex. Finally, Figure 3 contains a schematic potential energy profile for the processes in which a dhtp has been considered.

Tables 1 and 4 collect the relative energetic values of these complexes, while Tables 2, 3, and 5 contain the topological parameters of interest computed at the bond critical points (bcp's) and the overall NBO charge transfer between the HCOOH and HOO<sup>•</sup> units.

The topological analysis of the wave function according to the AIM theory by Bader<sup>36,37</sup> provides a powerful tool to analyze the bonding features in a molecule, and in particular, Koch and Popelier<sup>43</sup> reported a set of criteria, based on the AIM theory, to fully characterize the hydrogen-bond interactions. The electron density ( $\rho_{\text{bcp}}$ ) and the Laplacian of the electron density ( $\nabla^2\rho_{\text{bcp}}$ ) at the bcp's reveal the nature of the interactions. The  $\rho_{\text{bcp}}$  is related to the bond order and thus to the bond strength and it correlates well with the hydrogen-bond energy and the geometrical descriptors of the hydrogen bond strength. In

addition, the sign of  $\nabla^2\rho_{\text{bcp}}$  reveals whether charge is concentrated ( $\nabla^2\rho_{\text{bcp}} < 0$ ) as in covalent bonds or depleted ( $\nabla^2\rho_{\text{bcp}} > 0$ ) as in ionic bonds, hydrogen bonds, and van der Waals interactions.<sup>36,37,43</sup> For instance, Koch and Popelier report values in the range 0.02–0.04 au for  $\rho_{\text{bcp}}$  and 0.024–0.139 au for  $\nabla^2\rho_{\text{bcp}}$  for typical hydrogen bonds. It is also of interest to look at the energy density at the bcp, ( $H_{\text{bcp}}$ ), which is the sum of the kinetic electron energy density ( $G_{\text{bcp}}$ ) and the potential electron energy density ( $V_{\text{bcp}}$ ), and it was pointed out that if  $\nabla^2\rho_{\text{bcp}}$  is positive and  $H_{\text{bcp}}$  is negative, then the interaction is partially covalent in nature.<sup>44,45</sup> In addition, the ellipticity of a bond provides a measure of the extent to which the density is accumulated in a given plane, and therefore, it reflects the  $\pi$  character of the bond.<sup>36,37</sup> Finally, the overall NBO charge transfer has been evaluated by summing up the NBO atomic charges on either of the individual monomer, providing an estimation of the charge transferred between HCOOH and HOO<sup>•</sup> in the complex formation.

**Complexes Formed between *syn*-HCOOH and HOO<sup>•</sup>.** The most stable hydrogen-bond complex studied in this work is complex **1**, which has  $C_s$  symmetry ( $^2A'$ ) and has been recently and extensively reported in the literature.<sup>11,19,27</sup> Our results with respect to the geometrical parameters, energetic stability, and topological parameters of the corresponding wave function compare very well with those reported in the literature. Therefore, we will only discuss its main features. Figure 1 shows that complex **1** has a seven-member ring structure with two hydrogen bonds, one formed with the hydrogen of hydroperoxyl radical and the oxygen of carbonyl group (H3O2) with a computed hydrogen-bond distance of 1.643 Å and the other formed between the acidic hydrogen of HCOOH and the terminal oxygen of HO<sub>2</sub><sup>•</sup> radical (H1O4) with a computed hydrogen-bond length of 1.734 Å. Figure 1 also shows that the seven-member ring structure of this complex allows both hydrogen bonds to have a quite good directionality (with both O–H...O angles close to 167°), favoring the stability of the complex ( $\Delta H$  is 13.7 or 11.3 kcal/mol considering the BSSE corrections; see Table 1). The strength of both hydrogen bonds are also clearly reflected in the computed values of the topological parameters at the bcp's ( $\rho_{\text{bcp}} = 0.0532$  au and

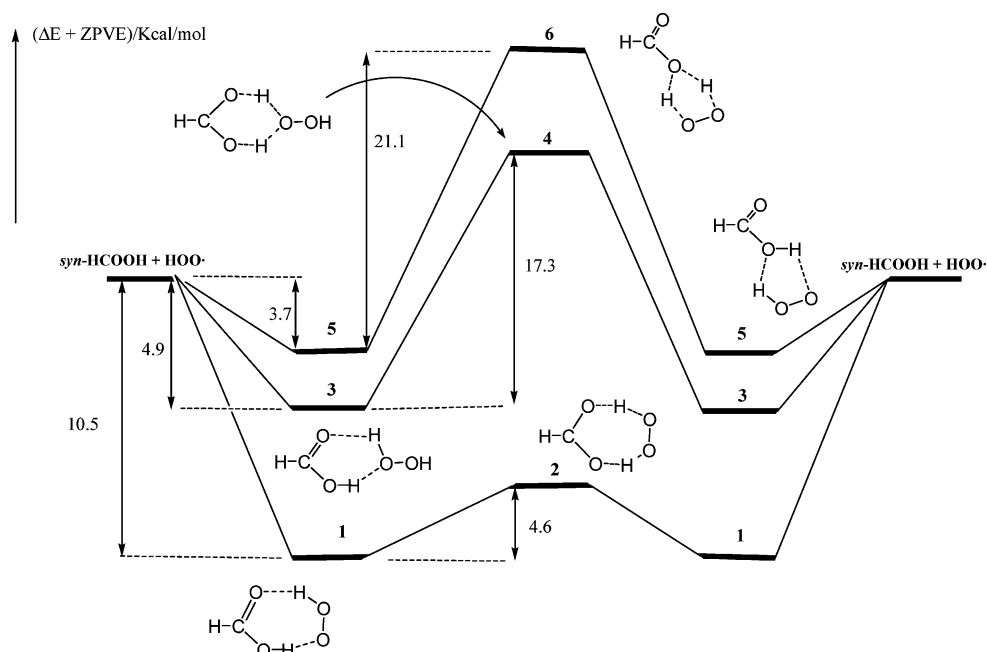


**Figure 3.** Schematic reaction energy profile for the different double proton transfer processes considered.

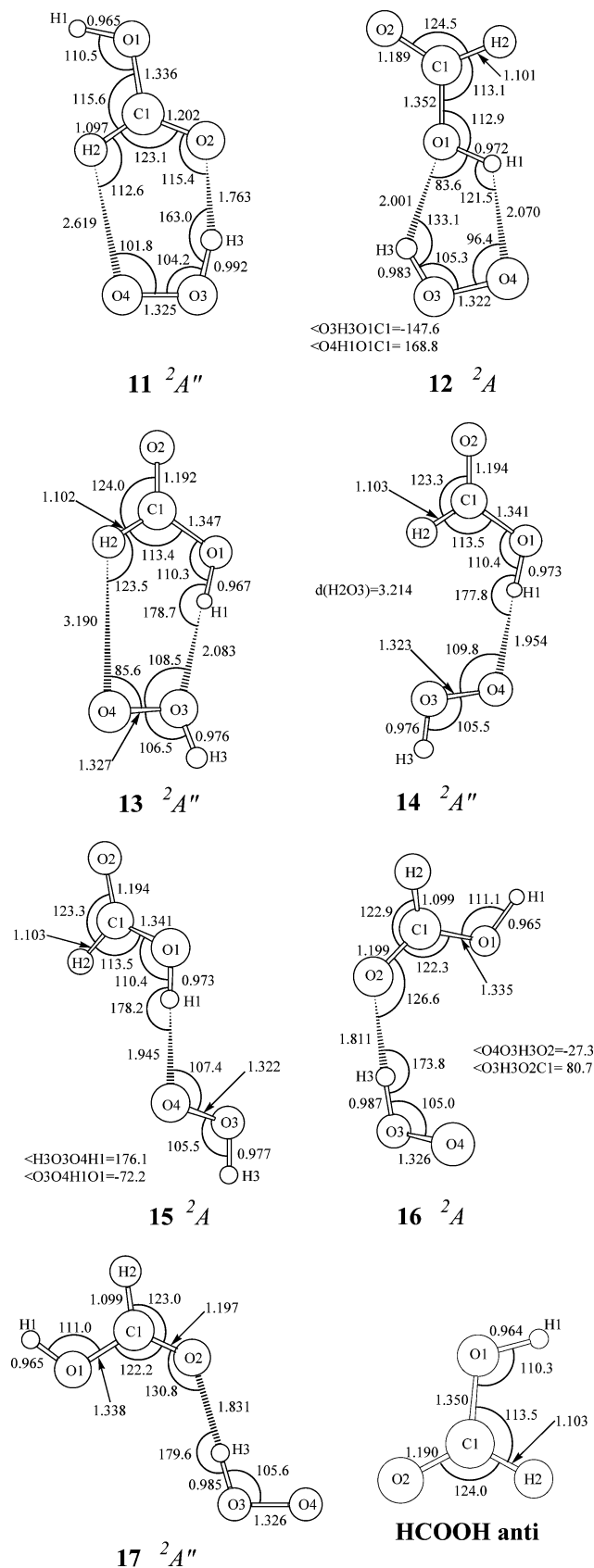


**Figure 4.** Selected geometrical parameters of the B3LYP/6-311+G(2df,2p)-optimized geometries for complexes formed between *anti*-HCOOH and HOO $\cdot$ . Distances are given in angstroms and angles in degrees.

$\nabla^2\rho_{\text{bcp}} = 0.1243$  au for H3O2 and  $\rho_{\text{bcp}} = 0.0441$  au and  $\nabla^2\rho_{\text{bcp}} = 0.1057$  au for H1O4; see Table 2), which are in line with the values reported by Parreira and Galembeck.<sup>19</sup> The smaller

**TABLE 1:** Calculated Zero-Point Vibrational Energies (ZPVE, kcal/mol), Absolute Entropies ( $S$ , eu), Relative Energies ( $\Delta E$ , kcal/mol), Relative Energies with ZPVE ( $\Delta E + \text{ZPVE}$ , kcal/mol), and Relative Enthalpies ( $\Delta H$ , kcal/mol) for Various Complexes between *syn*-HCOOH and OOH $\cdot$  Radical

structure	ZPVE <sup>a</sup>	$S^a$	$\Delta E^{b,c}$	CCSD(T)		
				$\Delta E + \text{ZPVE}^{b,c}$	$\Delta H^{b,c}$	
<i>syn</i> -HCOOH+OOH	30.0	114.0	0.00	0.00	0.00	
<b>1</b>	$^2A''$	32.4	77.4	-15.3	-12.9	-13.7
			(-12.9)	(-10.5)	(-11.3)	
<b>2<sup>d</sup></b>	$^2A_2$	28.9	71.5	-7.3	-8.3	-9.7
			(-)	(-)	(-)	
<b>3</b>	$^2A$	31.7	85.2	-8.1	-6.4	-6.5
			(-6.6)	(-4.9)	(-5.0)	
<b>4<sup>d</sup></b>	$^2A'$	28.7	74.5	12.3	10.9	9.7
			(-)	(-)	(-)	
<b>5</b>	$^2A''$	31.5	88.0	-6.4	-5.0	-5.0
			(-5.1)	(-3.7)	(-3.7)	
<b>6<sup>d</sup></b>	$^2A''$	28.4	79.6	17.7	16.1	15.2
			(-)	(-)	(-)	
<b>7</b>	$^2A''$	31.4	86.5	-6.4	-5.0	-4.9
			(-5.1)	(-3.8)	(-3.7)	
<b>8</b>	$^2A''$	31.8	84.3	-9.7	-7.9	-8.0
			(-8.3)	(-6.4)	(-6.6)	
<b>9</b>	$^2A$	31.3	89.1	-5.5	-4.2	-4.0
			(-4.3)	(-3.0)	(-2.8)	
<b>10</b>	$^2A$	30.6	98.8	-2.0	-1.5	-0.8
			(-1.6)	(-1.0)	(-0.3)	

<sup>a</sup> Values computed at the B3LYP/6-311+G(2df,2p) level of theory.

<sup>b</sup> Single point CCSD(T)/6-311+G(2df,2p) energies calculated at the B3LYP/6-311+G(2df,2p)-optimized geometries. <sup>c</sup> The values in parentheses include BSSE corrections computed at the CCSD(T)/6-311+G(2df,2p) level of theory. <sup>d</sup> Correspond to a transition state.

topological parameters of the bcp in the H1O4 hydrogen bond and its larger bond length, compared with those of H3O2, indicate that the former is weaker than the later, as pointed out by Francisco.<sup>11</sup> However, the relative short bond length of O4 $\cdot$ -H1 (1.734 Å) and the values of the density and Laplacian of the density at the bcp just discussed also point out that O4 is also a good acceptor. In addition, it is also worth mentioning the lengthening of the C1O2 bond (0.019 Å) and the shortening of the C1O1 and O3O4 bonds (0.033 and 0.007 Å, respectively) with respect to the separate reactants (see Figure 1). These changes in the bond lengths are also associated with significant changes in the ellipticities of the corresponding bonds. The results displayed in Table 3 point out that the ellipticity of the carbonyl bond (C1O2) is reduced by 0.023, whereas those of the C1O1 and O3O4 bonds are increased by 0.020 and 0.019, respectively, with respect to the reactants, indicating the delocalization of the  $\pi$  system and thus suggesting that complex **1** is stabilized by a resonance-assisted hydrogen bond (RAHB).<sup>61</sup> These data compare very well with those reported recently by Parreira and Galembeck,<sup>19</sup> who pointed also out the increase in the carbonyl group resonance. In addition, the values listed in Table 2 show that the total energy density  $H_{\text{bcp}}$  of the two hydrogen bonds (H3O2 and H1O4) are negative, which indicates that these hydrogen bonds are partially covalent in nature. Very recently Gora and co-workers<sup>46</sup> found also negative values of  $H_{\text{bcp}}$  for systems in which one expects RAHB to be formed.

Figure 2 displays the electron redistribution originating from the formation of two hydrogen bonds in **1**. It shows a redistribution of the electron density in regions along hydrogen bond axes where the electron density reduction (in gray) is concentrated at the positions of the hydrogen donors, while the electron density increase (in black) is observed at the positions of the hydrogen acceptors. These features are similar to those

**TABLE 2: Calculated Topological Properties of the Bond Critical Points of Interest<sup>a</sup> and NBO Net Atomic Charge Transfer<sup>b</sup> for the Complexes between *syn*-HCOOH and HOO• Radical**

structure	X–Y bond/ ring	$r_X$ (Å) <sup>c</sup>	$r_Y$ (Å) <sup>d</sup>	$\rho$ (au) <sup>e</sup>	$\nabla^2\rho$ (au) <sup>f</sup>	$G$ (au) <sup>g</sup>	$V$ (au) <sup>h</sup>	$H$ (au) <sup>i</sup>	$q_{\text{HCOOH}}$ (me) <sup>j</sup>
<b>1</b>	H3O2	0.530	1.115	0.0532	0.1243	0.0391	−0.0472	−0.0081	3.0
	H1O4	0.568	1.167	0.0441	0.1057	0.0315	−0.0365	−0.0050	
<b>2</b>	(3,1)	—	—	0.0110	0.0486	0.0110	−0.0099	0.0011	
	H3O2	0.289	0.910	0.1815	−0.4348	0.0874	−0.2835	−0.1961	
<b>3</b>	H3O3	0.304	0.933	0.1676	−0.3097	0.0835	−0.2444	−0.1609	19.3
	(3,1)	—	—	0.0165	0.0844	0.0190	−0.0169	0.0021	
<b>4</b>	H3O2	0.666	1.215	0.0311	0.0989	0.0124	−0.0107	0.0017	
	H1O3	0.805	1.328	0.0155	0.0565	0.0245	−0.0242	0.0002	
<b>5</b>	(3,1)	—	—	0.0107	0.0445	0.0099	−0.0087	0.0012	
	H3O2	0.251	0.884	0.2181	−0.9242	0.0832	−0.3975	−0.3143	
<b>6</b>	H3O3	0.361	0.969	0.1254	−0.0104	0.0755	−0.1536	−0.0781	
	(3,1)	—	—	0.0258	0.1495	0.0331	−0.0288	0.0043	
<b>7</b>	H3O1	0.763	1.262	0.0196	0.0787	0.0173	−0.0149	0.0024	−8.0
	H1O4	0.806	1.333	0.0189	0.0689	0.0155	−0.0138	0.0017	
<b>8</b>	(3,1)	—	—	0.0132	0.0682	0.0149	−0.0127	0.0022	
	H1O4	0.259	0.890	0.2176	−0.8770	0.0817	−0.3827	−0.3010	
<b>9</b>	H1O1	0.371	0.968	0.1259	−0.0062	0.0743	−0.1501	−0.0758	
	(3,1)	—	—	0.0471	0.3131	0.0704	−0.0626	0.0078	
<b>10</b>	H3O1	0.676	1.228	0.0261	0.0907	0.0212	−0.0197	0.0015	11.5
	H2O4	1.088	1.582	0.0073	0.0223	0.0050	−0.0043	0.0006	
<b>11</b>	(3,1)	—	—	0.0056	0.0251	0.0053	−0.0043	0.0010	
	H3O2	0.601	1.172	0.0375	0.1118	0.0294	−0.0309	−0.0015	
<b>12</b>	H2O4	1.118	1.586	0.0072	0.0246	0.0053	−0.0045	0.0008	30.2
	(3,1)	—	—	0.0066	0.0293	0.0062	−0.0051	0.0011	
<b>13</b>	H1O4	0.665	1.254	0.0264	0.0813	0.0199	−0.0195	0.0004	−29.1
<b>14</b>	H2O4	0.969	1.502	0.0091	0.0278	0.0062	−0.0055	0.0007	−8.6

<sup>a</sup> Determined from Bader topological analysis of the B3LYP/6-311+G(2df,2p) wave function. Atom numbering refers to Figure 1 and (3,1) stands for a bond critical point of ring type. <sup>b</sup> Determined from NBO population analysis of the B3LYP/6-311+G(2df,2p) wave function. <sup>c</sup> The distance between the bond critical point and the X atom. <sup>d</sup> The distance between the bond critical point and the Y atom. <sup>e</sup> Electronic charge density at the bond critical point. <sup>f</sup> Laplacian of the electron density at the bond critical point. <sup>g</sup> Kinetic electron energy density at the bond critical point. <sup>h</sup> Potential electron energy density at the bond critical point. <sup>i</sup> Electron energy density at the bond critical point. <sup>j</sup> Net charge (in millielectrons) over the HCOOH moiety.

**TABLE 3: Calculated Ellipticities ( $\epsilon$ ) at the Bond Critical Points for Formic Acid, Hydroperoxyl Radical, and Complex 1**

bond <sup>a</sup>	HCOOH	HOO•	<b>1</b>
C1O1	0.0111	—	0.0315
O1H1	0.0125	—	0.0084
C1O2	0.1289	—	0.1062
O3O4	—	0.0166	0.0353
O3H3	—	0.0272	0.0218
H3O2	—	—	0.0142
H1O4	—	—	0.0459
H1O3	—	—	—

<sup>a</sup> Atom numbering according to Figure 1.

reported recently for HOO••H<sub>2</sub>SO<sub>4</sub><sup>18</sup> and HO••HCOOH<sup>25</sup> complexes and visualize clearly the well-known fact that there is a charge transfer (electrons transfer) associated with a hydrogen bond whose direction is reverse to the direction of proton donation.<sup>7</sup> In fact, Figure 2 agrees with the double charge transfer associated with the two hydrogen bonds going in opposite directions. This double charge transfer results in a very small net charge transfer of 3 me over the HCOOH, as computed after an NBO analysis and displayed in Table 2. In addition, Figure 2 shows also that the electron redistribution associated with the two hydrogen bonds goes beyond the two O–H••O hydrogen bonds so that it affects directly the two CO bonds and the OO bond, as shown by the changes in the respective bond lengths and in the values of the ellipticities discussed above. In a similar way to the intermolecular hydrogen bonds in dimers of formic acid, acetic acid, and formamide recently reported by Gora and co-workers,<sup>46</sup> the electron redistribution displayed in Figure 2, mainly with respect to the changes in

**TABLE 4: Calculated Zero-Point Vibrational Energies (ZPVE, kcal/mol), Absolute Entropies ( $S$ , eu), Relative Energies ( $\Delta E$ , kcal/mol), Relative Energies with ZPVE ( $\Delta E + \text{ZPVE}$ , kcal/mol), and Relative Enthalpies ( $\Delta H$ , kcal/mol) for Various Complexes between *anti*-HCOOH and HOO• Radical**

structure	ZPVE <sup>a</sup>	$S^a$	CCSD(T)			
			$\Delta E^{b,c}$	$\Delta E + \text{ZPVE}^{b,c}$	$\Delta H^{b,c}$	
<i>anti</i> -HCOOH+OOH	29.8	114.1	0.00	0.00	0.00	
<b>11</b>	<sup>2</sup> A''	31.7	84.0	−10.3	−8.4	−8.6
				(−8.9)	(−7.0)	(−7.2)
<b>12</b>	<sup>2</sup> A	31.4	86.7	−8.0	−6.4	−6.5
				(−6.6)	(−5.0)	(−5.1)
<b>13</b>	<sup>2</sup> A''	30.7	93.5	−4.5	−3.6	−3.1
				(−3.6)	(−2.8)	(−2.2)
<b>14</b>	<sup>2</sup> A''	31.1	91.9	−6.1	−4.9	−4.6
				(−5.1)	(−3.8)	(−3.5)
<b>15</b>	<sup>2</sup> A	31.1	91.8	−6.1	−4.8	−4.5
				(−5.0)	(−3.8)	(−3.5)
<b>16</b>	<sup>2</sup> A	31.4	88.2	−8.5	−6.9	−6.8
				(−7.2)	(−5.6)	(−5.5)
<b>17</b>	<sup>2</sup> A''	31.3	82.9	−7.9	−6.4	−6.9
				(−6.7)	(−5.2)	(−5.7)

<sup>a</sup> Values computed at the B3LYP/6-311+G(2df,2p) level of theory. <sup>b</sup> Single-point CCSD(T)/6-311+G(2df,2p) energies calculated at the B3LYP/6-311+G(2df,2p)-optimized geometries. <sup>c</sup> The values in parentheses include BSSE corrections computed at the CCSD(T)/6-311+G(2df,2p) level of theory.

the electron density associated with the two CO bonds of the formic acid moiety, supports the features of the intermolecular RAHB systems.

Viewing complex **1** as an incipient step of a proton-transfer reaction, as pointed out by Steiner,<sup>7</sup> let us investigate the dhtp

between HCOOH and HOO<sup>•</sup>. The reaction involves the simultaneous transfer of the acidic hydrogen of formic acid to the terminal oxygen of the hydroperoxyl radical and the hydrogen of HO<sub>2</sub><sup>•</sup> radical moiety to the oxygen of the carbonyl group of HCOOH, so that the fate of the reaction is also complex **1**. The corresponding transition state has been depicted as structure **2** in Figure 1 and has C<sub>2v</sub> symmetry. The analysis of the wave function shows that the electronic state is <sup>2</sup>A<sub>2</sub> and the electron density associated with the unpaired electron is perpendicular to the molecular plane, so it does not take part in the reaction, and consequently, the process clearly involves a double proton transfer. The geometrical parameters of this transition state show that both hydrogens are slightly closer to the oxygens of the formic acid moiety (H1O1 and H3O2 = 1.198 Å) than to the oxygens of the hydroxyperoxyl moiety (H1O4 and H3O3 = 1.237 Å), which is also reflected in the topological parameter of the wave function (see Table 2). In addition, the two CO bond lengths are equal (1.261 Å) and halfway between the length of a single and a double bond, which points out a delocalization of the π system in the formic acid moiety. From an energetic point of view, our calculations displayed in Table 1 predict a sizable potential energy barrier of 8.0 kcal/mol with respect to complex **1**. Taking into account the ZPVE (see Table 1 and Figure 3), this barrier will be reduced to the value of 4.6 kcal/mol at 0 K (a 43% of reduction). Figure 3 shows also that, because of the large stability of **1**, the transition state **2** lies about 6 kcal/mol below the sum of the energies of the separate reactants.

Complex **3** has a six-member ring structure (see Figure 1). It is bonded by two hydrogen bonds in which the O3 of the hydroperoxyl radical moiety acts as a donor and as acceptor simultaneously. This geometrical constraint produces more bended O<sup>•</sup>H–O interactions (140.4° and 145.0° on the donor side and 114.8° and 83.2° on the acceptor side) than in **1**, resulting in a much weaker stability (Δ*H* = 6.5 or 5.0 kcal/mol, taking into account the BSSE corrections). This six-member ring structure resembles very much the most stable hydrogen-bond complex formed between formic acid and hydroxyl radical,<sup>25</sup> which differentiates from **3** in the fact that the hydrogen of the radical moiety has been substituted by an OH group. Here, the terminal oxygen (O4) of the HO<sub>2</sub> radical moiety in complex **3** (see Figure 1) does not participate directly in the hydrogen-bond interaction, but its electronegative character produces a destabilizing inductive effect (complex **3** is about 1 kcal/mol less stable than structure **5** in the HCOOH<sup>•</sup>HO complex). This inductive effect involves a small, but significant, change in the lengths of the two hydrogen bonds of complex **3** (*d*<sub>O2–H3</sub> = 1.876 Å and *d*<sub>O3–H1</sub> = 2.131 Å), which are shorter and larger, respectively, than the corresponding distances of structure **5** in HCOOH<sup>•</sup>HO complex.<sup>25</sup>

As in the case of formic acid plus hydroxyl radical complex,<sup>25</sup> we can envisage a dhtp in **3** that involves the transfer of the hydrogen of the hydroxyl group of HCOOH to the oxygen of HO<sub>2</sub><sup>•</sup> radical and simultaneously the transfer of the hydrogen of the hydroperoxyl group to the oxygen of the carbonyl, so that the reactants and products are the same species (complex **3**). This transition structure has been labeled as **4** in Figure 1. It has a six-member ring structure and possesses C<sub>s</sub> symmetry, where the molecular plane bisects the molecule. The electronic state is <sup>2</sup>A', so that the unpaired electron does not take part in the dhtp as in the case of **2** (see just above). Our results (Figure 3) predict an energy barrier for this process of 17.3 kcal/mol at 0 K (relative to complex **3**). Again, this six-member ring transition structure resembles very much the dhtp described for

the HCOOH plus HO reaction (see TS3 in reference <sup>21</sup>), although the activation barrier was computed to be about 5 kcal/mol smaller in the formic acid plus HO<sup>•</sup> radical, pointing out clearly the destabilization effect produce by O4, as indicated above for **3**.

Complex **5** has a five-member ring structure in which the hydroxyl group of the formic acid moiety acts simultaneously as hydrogen donor and as acceptor, whereas the O4 and O3 of the hydroperoxyl radical moiety act as acceptor and as donor, respectively. The stability of this complex has been computed to be 5.0 kcal/mol (Δ*H*(298) = 3.7 kcal/mol, considering the BSSE corrections), which is smaller than those computed for **1** and **3**. This smaller stability can be attributed to the geometrical constraint imposed by the five-member ring structure and also to the smaller acceptor ability of the oxygen of the hydroxyl group (O1). According to the stability of this complex, our calculations predict larger distances for the two hydrogen bonds as well as smaller values for the topological parameters of the wave function at the corresponding bcp (2.133 Å, ρ<sub>bcp</sub> = 0.0189 au, and ∇<sup>2</sup>ρ<sub>bcp</sub> = 0.0689 au for H1O4 and 2.024 Å, ρ<sub>bcp</sub> = 0.0196 au, and ∇<sup>2</sup>ρ<sub>bcp</sub> = 0.0787 au for H3O1; see Figure 1 and Table 2) than those reported for **1** and **3**.

As for the two previous complexes discussed above (**1** and **3**), there is also a dhtp with its corresponding transition state, structure **6** in Figure 1. It is a symmetric (C<sub>s</sub>) five-member ring and its electronic characterization is <sup>2</sup>A'' (the electron density of the unpaired electron is shared between O3 and O4 and is perpendicular to the double proton transfer direction). From an energetic point of view, our results displayed in Table 1 and Figure 3 predict a high activation barrier for this process (21.1 kcal/mol at 0 K), according to the strained geometry derived from the five-member ring structure.

We have also found two complexes having six-member ring structures with two hydrogen bonds that are formed between the *syn*-HCOOH and HOO<sup>•</sup> moieties (structures **7** and **8**). One hydrogen bond is formed between the formyl hydrogen and the terminal oxygen of hydroperoxyl radical (H2O4) and the other hydrogen bond is formed between the hydrogen of the HOO<sup>•</sup> moiety and the oxygen of the hydroxyl group in **7** (H3O1) or between the hydrogen of the HOO<sup>•</sup> moiety and the oxygen of the carbonyl group in **8** (H3O2). From an energetic point of view, we have computed both complexes to be 3.7 and 6.6 kcal/mol more stable than the reactants (Δ*H*(298) values, including BSSE corrections). Moreover, it is also interesting to remark that complex **8** is computed to be 3 kcal/mol more stable than complex **7**, which points out clearly that the carbonyl oxygen forms stronger hydrogen bonds than the hydroxyl oxygen. This higher stability of **8** results in a much shorter length of the hydrogen bond (1.771 Å for H3O2 in **8** versus 1.904 Å for H3O1 in **7**), while the H2O4 bond length is quite the same in both complexes (2.7 Å). In addition, these differences in the hydrogen bond strengths are also clearly reflected in the values of the topological parameters at the corresponding bcp's, as displayed in Table 2. Thus, whereas we have computed quite similar topological values for H2O4 (ρ<sub>bcp</sub> = 0.0073 au and ∇<sup>2</sup>ρ<sub>bcp</sub> = 0.0223 au for **7** and ρ<sub>bcp</sub> = 0.0072 au and ∇<sup>2</sup>ρ<sub>bcp</sub> = 0.0246 au for **8**), a larger value of the density and its Laplacian is obtained for H3O2 in **8** (ρ<sub>bcp</sub> = 0.0375 au and ∇<sup>2</sup>ρ<sub>bcp</sub> = 0.1118 au) than for H3O1 in **7** (ρ<sub>bcp</sub> = 0.0261 au and ∇<sup>2</sup>ρ<sub>bcp</sub> = 0.0907 au). These results indicate clearly that H3O2 is a stronger hydrogen bond than H3O1, as pointed out above; i.e., the oxygen of a carbonyl group is a better acceptor than the oxygen of a hydroxyl group. It is also interesting to observe from Table 2 that, although close to zero, a negative value (−0.0015) of *H*<sub>bcp</sub>

**TABLE 5: Calculated Topological Properties of the Bond Critical Points of Interest<sup>a</sup> and NBO Net Atomic Charge Transfer<sup>b</sup> for the Complexes between *anti*-HCOOH and HOO• Radical**

structure	X–Y bond/ ring	$r_X$ (Å) <sup>c</sup>	$r_Y$ (Å) <sup>d</sup>	$r$ (au) <sup>e</sup>	$\nabla^2\rho$ (au) <sup>f</sup>	$G$ (au) <sup>g</sup>	$V$ (au) <sup>h</sup>	$H$ (au) <sup>i</sup>	$q_{\text{HCOOH}}$ (me) <sup>j</sup>
<b>11</b>	H3O2	0.596	1.168	0.0384	0.1132	0.0300	−0.0318	−0.0017	31.4
	H2O4	1.073	1.553	0.0082	0.0274	0.0060	−0.0052	0.0008	
<b>12</b>	(3,1)	—	—	0.0072	0.0322	0.0069	−0.0058	0.0011	−9.9
	H3O1	0.751	1.251	0.0209	0.0835	0.0186	−0.0162	0.0023	
	H1O4	0.772	1.303	0.0216	0.0785	0.0179	−0.0162	0.0017	
<b>13</b>	(3,1)	—	—	0.0143	0.0752	0.0164	−0.0139	0.0024	−9.7
	H1O3	0.766	1.317	0.0157	0.0601	0.0129	−0.0109	0.0021	
	H2O4	1.378	1.815	0.0024	0.0091	0.0018	−0.0013	0.0005	
<b>14</b>	(3,1)	—	—	0.0024	0.0107	0.0020	−0.0014	0.0006	−25.6
	H1O4	0.684	1.270	0.0244	0.0775	0.0185	−0.0177	0.0008	
<b>15</b>	H1O4	0.679	1.266	0.0251	0.0791	0.0190	−0.0183	0.0007	−26.8
<b>16</b>	H3O2	0.622	1.190	0.0328	0.1031	0.0258	−0.0259	−0.0001	29.5
<b>17</b>	H3O2	0.632	1.199	0.0309	0.0996	0.0245	−0.0241	0.0004	27.1

<sup>a</sup> Determined from Bader topological analysis of the B3LYP/6-311+G(2df,2p) wave function. Atom numbering refers to Figure 1 and (3,1) stands for a bond critical point of ring type. <sup>b</sup> Determined from NBO population analysis of the B3LYP/6-311+G(2df,2p) wave function. <sup>c</sup> The distance between the bond critical point and the X atom. <sup>d</sup> The distance between the bond critical point and the Y atom. <sup>e</sup> Electronic charge density at the bond critical point. <sup>f</sup> Laplacian of the electron density at the bond critical point. <sup>g</sup> Kinetic electron energy density at the bond critical point. <sup>h</sup> Potential electron energy density at the bond critical point. <sup>i</sup> Electron energy density at the bond critical point. <sup>j</sup> Net charge (in millielectrons) over the HCOOH moiety.

is obtained for the H3O2 hydrogen bond, indicating the slight covalent nature of this interaction, which agrees with the relative high stability ( $\Delta H = 6.6$  kcal/mol; see Table 1) computed for this complex.

The latest two complexes between *syn*-HCOOH and HOO• (**9** and **10**) are held both by only one hydrogen bond. The complex **9** is formed between the acidic hydrogen and the terminal oxygen of the HOO• moiety with a computed bond length of 1.918 Å (H1O4) and a stability of 2.8 kcal/mol with respect to the separate reactants ( $\Delta H(298)$  value, including the BSSE correction). Here it is worth noting that a hydrogen bond between H1 and O4 is also described in **1**, although in that case we have obtained a bond length 0.18 Å smaller (see above and Figure 1). This result suggests a stronger H1O4 hydrogen bond in **1**, instead of the fact that the linearity is worse (O1H1O4 = 167.7° in **1** compared to 176.2° value for the same angle in **9**). This conclusion is also supported by larger values of the density and Laplacian of the density at the bcp in **1** than in **9** for the H1O4 hydrogen bond (see Table 2). The fact that the H1O4 hydrogen bond is stronger in **1** can be attributed to the resonance effect previously described in complex **1**. Finally, the hydrogen bond in complex **10** is formed between the formyl hydrogen, the worst hydrogen donor of the formic acid, and the terminal oxygen of the HOO• moiety and, accordingly, is the least stable complex studied in this work ( $\Delta H(298) = 0.3$  kcal/mol, considering the BSSE corrections).

In addition, it is interesting to comment on the charge transfer between the two moieties of each hydrogen-bonded complex (*syn*-formic acid and hydroperoxyl radical). It is well-known that the electronic reorganization derived from the formation of a hydrogen bond is associated with a charge transfer between the two moieties of the complex and that the direction of the electron transfer is reverse to the direction of the proton donation.<sup>7</sup> The corresponding NBO computed values ( $\Delta q$  over the HCOOH) displayed in Table 2 show a net electron transfer over HOO radical for complexes **1**, **3**, **7**, and **8** and a net electron transfer over HCOOH for **5**, **9**, and **10**, pointing out that HCOOH can act as Lewis acid or Lewis base with respect to HOO radical, depending on how both molecules approach each other. Complexes **1**, **3**, **5**, **7**, and **8** have two hydrogen bridges and there is a double charge transfer from HCOOH to HO<sub>2</sub>• radical and from HO<sub>2</sub>• radical to HCOOH. The corresponding

values displayed in Table 2 refer to the net charge transfer, including the charge transfer associated with the two hydrogen bonds. Thus, since the charge transfer in a given hydrogen bond may be related to its strength, in these double hydrogen-bonded complexes, a large value in the charge transfer between two moieties reflects a larger difference in the strengths of the two respective hydrogen bonds.

**Complexes Formed between *anti*-HCOOH and HOO•.** For the sake of completeness, we have also investigated the hydrogen-bonded complexes formed between *anti*-HCOOH and HO<sub>2</sub>• radical. We have found seven stationary points, and among them, three display a cyclic structure (complexes **11**, **12**, and **13**), while the remaining four (structures **14**, **15**, **16**, and **17**) have only one hydrogen bond. In general these hydrogen-bonded complexes present the same features analyzed above, so we will only discuss briefly these complexes.

Complexes **11** and **12** have the same kind of hydrogen bridges as complexes **8** and **5**, respectively. For instance, complexes **11** and **8** differentiate in the relative orientation of the hydroxyl group of the formic acid moiety (*anti* or *syn*), which does not participate in any of the two hydrogen bonds. Accordingly, their stabilities are very similar ( $\Delta H(298)$  about 7 kcal/mol, considering the BSSE corrections; see Tables 1 and 4), as are their geometrical structures and topological parameters of their wave function (see Tables 2 and 5 and Figures 1 and 4).

Complex **13** (see Figure 4) is the less stable one having a cyclic structure ( $\Delta H(298) = 2.2$  kcal/mol, taking into account the BSSE corrections). In this case, the two hydrogen donor groups (C1 and O1) belong to the formic acid moiety, whereas the two acceptors (O4 and O3) are from the HO<sub>2</sub>• radical moiety, so that we face the very unfavorable situation in which the worst donor (C1H2••O4) coexists with a bad acceptor (O3••H1O1). According to this small stability, it presents very large hydrogen-bond distances and, accordingly, very small values of the topological parameters at the bcp's (see Table 5).

Finally, the remaining complexes having one hydrogen bond, **14** and **15**, are two conformers around the O1H1••O4 hydrogen bond, which takes place between the hydrogen of the hydroxyl group of the formic acid moiety and the terminal oxygen of the HO<sub>2</sub> radical. Therefore, their hydrogen-bond lengths (close to 1.95 Å), stabilities ( $\Delta H(298) = 3.5$  kcal/mol, taking into account the BSSE corrections), and topological parameters of the

corresponding wave functions are very similar and also comparable to the corresponding parameters of complex **9** with the same hydrogen-bond interaction. Similarly, complexes **16** and **17** are held together by one hydrogen bond involving the carbonyl oxygen as acceptor group and by HO<sub>2</sub><sup>•</sup> radical as donor. They are also two conformers that differentiate from each other by a rotation through the O2<sup>•</sup>–H3O3 hydrogen bond, and consequently, their stability (about 5.7 kcal/mol), bond distances (1.811 and 1.831 Å, respectively), and topological parameters of their wave functions are very similar.

At this point, it is finally worth pointing out that the hydrogen-bond interactions of complexes **14** and **15** (O1H1<sup>•</sup>–O4, with a computed stability close to 3.5 kcal/mol) and complexes **16** and **17** (O3H3<sup>•</sup>–O2, with a computed stability close to 5.7 kcal/mol) are separately the two interactions involved in the formation of the most stable complex **1**. Therefore, these results allow us to estimate indirectly the extra stabilization produced in **1** by the formation of a ring as a consequence of the simultaneous occurrence of the two hydrogen bonds. The sum of the two interactions as computed for **14** plus **16** (or **15** plus **17**) amounts 9.2 kcal/mol ( $\Delta H$  values, see Table 4), a value that is smaller than the 11.3 kcal/mol computed for **1** ( $\Delta H$  value, Table 1). Thus, we can conclude that the extra stabilization produced in **1** by the formation of a ring can be estimated in a value close to 2 kcal/mol. It is worth noting that complex **1** is extra stabilized by the concurrence of a resonance effect of the  $\pi$  system according to the RAHB mechanism, as discussed above. This effect alone would probably be greater than the estimated 2 kcal/mol, but the formation of ring in **1** imposes a geometric restriction in both OH<sup>•</sup>–H hydrogen bonds with angles close to 167°, which produces a destabilization effect.

#### IV. Summary and Conclusions

A systematic theoretical study on the stability, structure, and electronic features of 17 stationary points involving hydrogen-bonded complexes between *syn*- and *anti*-HCOOH with HO<sub>2</sub><sup>•</sup> radical in the gas phase has been reported. Between them, 11 complexes present a cyclic structure possessing two hydrogen bond interactions, where three of them have been characterized as transition states.

Complexes **9**, **10**, **14**, **15**, **16**, and **17** are held together by a single hydrogen bond and their stabilities vary from 0.3 to 5.7 kcal/mol, depending on the different groups involved in the hydrogen-bond interaction; e.g., the oxygen of the carbonyl group is a much better acceptor than the oxygen of the hydroxyl group of formic acid. According to the strength of the different hydrogen bonds observed, the computed hydrogen bond lengths change from 1.811 to 2.471 Å.

Complexes **1**, **3**, **5**, **7**, **8**, **11**, **12**, and **13** possess cyclic structure with two hydrogen bonds. Their stabilities vary among 2.2 and 11.3 kcal/mol, depending on several factors, such as the groups involved in the hydrogen-bond interaction, the geometrical constraints derived from the ring formation (seven-member ring for **1**; six-member ring for **3**, **7**, **8**, **11**, and **13**; and five-member ring for **5** and **12**), and the relative orientation of both moieties (HCOOH and HOO<sup>•</sup>). In addition, there is a concurrence of further stabilizing effects such as RAHB, as in the case of **1**, where the  $\pi$  bond of the carbonyl group can be delocalized through the OCOH skeleton of the formic acid moiety, or even an inductive effect as in the case of **3**. The quantification of these different effects is very difficult, and they can operate in opposite directions (as the geometrical constraints and RAHB effects). However, our systematic study has allowed us to estimate the extra stabilization produced in **1**, due to the RAHB mechanism by the formation of a ring, as about 2 kcal/mol.

Structures **2**, **4**, and **6** have been characterized as transition states involving, each of them, a dhtp from **1**, **3**, and **5**, respectively, so that, in each case, the product is the same hydrogen-bonded complex as the reactant. The corresponding activation barriers (at 0 K) have been computed to be 4.6 kcal/mol for **2** relative to **1**, 17.3 kcal/mol for **4** relative to **3**, and 21.1 kcal/mol for **6** relative to **5**. These different activation barriers depend also on the same effects as described in the previous point.

A systematic analysis of the hydrogen-bonded complexes reported in the present work shows that all structures possessing the same kind of donor–acceptor interactions have very similar features, regarding their energetic stability, hydrogen-bond distances, and topological parameters of their wave function. In addition, the values of the topological parameters of the wave function computed at the respective bcp's change according to the strength of the bond, from  $\rho_{\text{bcp}} = 0.0532$  au and  $\nabla^2\rho_{\text{bcp}} = 0.1243$  au for H3O2 in the most stable complex **1** to  $\rho_{\text{bcp}} = 0.0091$  au and  $\nabla^2\rho_{\text{bcp}} = 0.0278$  au for H2O4 in the most labile single hydrogen-bonded complex **10**. Moreover, the computed negative values for the electronic energy density of several hydrogen bonds in complexes **1**, **8**, and **11** indicated that they are partially covalent in nature. It is worth also noting the fact that the charge-transfer estimation, based on the NBO analysis, indicates that HCOOH can act as Lewis acid or as Lewis basis with respect to HO<sub>2</sub><sup>•</sup> radical, depending on how both moieties interact with each other.

**Acknowledgment.** The financial support for this work was provided by the Dirección General de Investigación Científica y Técnica (DGICYT, grant CTQ2005-07790) and by the Generalitat de Catalunya (Grant 2005SGR00111). M.T. is thankful for the financial support by C.S.I.C. through Beca de Introducció a la Investigació (B.O.E. 29-07-1999). The calculations described in this work were performed at the Centre de Supercomputació de Catalunya (CESCA) and the Centro de Supercomputación de Galicia (CESGA), whose services are gratefully acknowledged.

**Supporting Information Available:** Absolute energies, enthalpies, and the Cartesian coordinates of all structures reported in this paper. This material is available free of charge via Internet at <http://pubs.acs.org>

#### References and Notes

- (1) Jeffrey, G. A.; Saenger, W. *Hydrogen Bonding in Biological Structures*; Springer-Verlag: Berlin, 1991.
- (2) Scheiner, S. *Hydrogen Bonding, A Theoretical Perspective*; Oxford University Press: Oxford, 1997.
- (3) Schuster, P. *Hydrogen Bonds*; Springer-Verlag: Berlin, 1984; Vol. 120.
- (4) Guerra, C. F.; Bickelhaupt, F. M. *Angew. Chem., Int. Ed.* **1999**, *38*, 2942.
- (5) Hobza, P.; Havlas, Z. *Chem. Rev.* **2000**, *100*, 4253.
- (6) Prins, L. J.; Reinhoudt, D. N.; Timmerman, P. *Angew. Chem., Int. Ed.* **2001**, *40*, 2383.
- (7) Steiner, T. *Angew. Chem., Int. Ed.* **2002**, *41*, 48.
- (8) Wormer, P. E. S.; van der Avoird, A. *Chem. Rev.* **2000**, *100*, 4109.
- (9) Aloisio, S.; Francisco, J. S. *J. Phys. Chem. A* **2000**, *104*, 3211.
- (10) Aloisio, S.; Francisco, J. S. *Acc. Chem. Res.* **2000**, *33*, 825.
- (11) Aloisio, S.; Francisco, J. S. *J. Am. Chem. Soc.* **2000**, *122*, 9196.
- (12) Chakraborty, D.; Park, J.; Lin, M. C. *Chem. Phys.* **1998**, *231*, 39.
- (13) delValle, C. P.; Valdemoro, C.; Novoa, J. J. *J. Mol. Struct. (THEOCHEM)* **1996**, *371*, 143.
- (14) Aloisio, S.; Francisco, J. S. *J. Phys. Chem. A* **1998**, *102*, 1899.
- (15) Aloisio, S.; Francisco, J. S. *J. Phys. Chem. A* **1999**, *103*, 6049.
- (16) Aloisio, S.; Francisco, J. S. *J. Phys. Chem. A* **2003**, *107*, 2492.
- (17) Francisco, J. S. *Angew. Chem., Int. Ed.* **2000**, *39*, 4570.
- (18) Miller, C. E.; Francisco, J. S. *J. Am. Chem. Soc.* **2001**, *123*, 10387.



- (19) Parreira, R. L. T.; Galembeck, S. E. *J. Am. Chem. Soc.* **2003**, *125*, 15614.
- (20) Zhou, Z. Y.; Qu, Y. H.; Gu, L.; Gao, H. W.; Cheng, X. L. *J. Mol. Struct. (THEOCHEM)* **2002**, *586*, 149.
- (21) Anglada, J. M. *J. Am. Chem. Soc.* **2004**, *126*, 9809.
- (22) Flowers, B. A.; Szalay, P. G.; Stanton, J. F.; Kallay, M.; Gauss, J.; Csaszar, A. G. *J. Phys. Chem. A* **2004**, *108*, 3195.
- (23) Solimannejad, M.; Azimi, G.; Pejov, L. *Chem. Phys. Lett.* **2004**, *400*, 185.
- (24) Solimannejad, M.; Azimi, G.; Pejov, L. *Chem. Phys. Lett.* **2004**, *391*, 201.
- (25) Torrent-Sucarrat, M.; Anglada, J. M. *ChemPhysChem* **2004**, *5*, 183.
- (26) Wang, B.; Hou, H. *Chem. Phys. Lett.* **2005**, *410*, 235.
- (27) Hansen, J. C.; Francisco, J. S. *ChemPhysChem* **2002**, *3*, 833.
- (28) Frey, P. A. *Chem. Rev.* **1990**, *90*, 1343.
- (29) Stubbe, J.; van der Donk, W. A. *Chem. Rev.* **1998**, *98*, 705.
- (30) Espinosa-Garcia, J. *J. Am. Chem. Soc.* **2004**, *126*, 920.
- (31) Qu, Y.; Bian, X.; Zhou, Z.; Gao, H. *Chem. Phys. Lett.* **2002**, *366*, 260.
- (32) Legrand, M.; Angelis, M. d. *J. Geophys. Res.* **1995**, *100*, 1445.
- (33) Granby, K.; Christensen, C. S.; Lohse, C. *Atmos. Environ.* **1997**, *31*, 1403.
- (34) Kesselmeier, J. *J. Atmos. Chem.* **2001**, *39*, 219.
- (35) Heard, D. E.; Pilling, M. J. *Chem. Rev.* **2003**, *103*, 5163.
- (36) Bader, R. F. W. *Atoms in Molecules: A Quantum Theory*; Clarendon: Oxford, 1990.
- (37) Bader, R. F. W. *Chem. Rev.* **1991**, *91*, 893.
- (38) Reed, A. E.; Curtiss, L. A.; Weinhold, F. *Chem. Rev.* **1988**, *88*, 899.
- (39) Rozas, I.; Alkorta, I.; Elguero, J. *J. Am. Chem. Soc.* **2000**, *122*, 11154.
- (40) Guerra, C. F.; Bickelhaupt, F. M. *Angew. Chem., Int. Ed.* **1999**, *38*, 2942.
- (41) Grabowski, S. J. *J. Phys. Chem. A* **2001**, *105*, 10739.
- (42) Popelier, P. L. A. *J. Phys. Chem. A* **1998**, *102*, 1873.
- (43) Koch, U.; Popelier, P. L. A. *J. Phys. Chem.* **1995**, *99*, 9747.
- (44) Cremer, D.; Kraka, E. *Angew. Chem., Int. Ed. Engl.* **1984**, *23*, 627.
- (45) Jenkins, S.; Morrison, I. *Chem. Phys. Lett.* **2000**, *317*, 97.
- (46) Gora, R. W.; Grabowski, S. J.; Leszczynski, J. *J. Phys. Chem. A* **2005**, *109*, 6397.
- (47) Ziolkowski, M.; Grabowski, S. J.; Leszczynski, J. *J. Phys. Chem. A* **2006**, *110*, 6514.
- (48) Frisch, M. J.; Trucks, G. W.; Schlegel, H. B.; Scuseria, G. E.; Robb, M. A.; Cheeseman, J. R.; Zakrzewski, V. G.; Montgomery, J. A.; Stratmann, R. E.; Burant, J. C.; Dapprich, S.; Millam, J. M.; Daniels, A. D.; Kudin, K. N.; Strain, M. C.; Farkas, O.; Tomasi, J.; Barone, V.; Cossi, M.; Cammi, R.; Mennucci, B.; Pomelli, C.; Adamo, C.; Clifford, S.; Ochterski, J.; Petersson, G. A.; Ayala, P. Y.; Cui, Q.; Morokuma, K.; Salvador, P.; Dannenberg, J. J.; Malick, D. K.; Rabuck, A. D.; Raghavachari, K.; Foresman, J. B.; Cioslowski, J.; Ortiz, J. V.; Baboul, A. G.; Stefanov, B. B.; Liu, G.; Liashenko, A.; Piskorz, P.; Komaromi, I.; Gomperts, R.; Martin, R. L.; Fox, D. J.; Keith, T.; Al-Laham, M.; Peng, C.; Nanayakkara, A.; Challacombe, M.; Gill, P. M. W.; Johnson, B. G.; Chen, W.; Wong, M. W.; Andres, J. L.; Gonzalez, R.; Head-Gordon, M.; Replogle, E. S.; Pople, J. A. *Gaussian* 98, rev. A11; Gaussian: Pittsburgh, PA, 1998.
- (49) Krishnan, R.; Binkley, J. S.; Seeger, R.; Pople, J. A. *J. Chem. Phys.* **1980**, *72*, 650.
- (50) Becke, A. D. *J. Chem. Phys.* **1993**, *98*, 5648.
- (51) Cizek, J. *J. Chem. Phys.* **1966**, *45*, 4256.
- (52) Lee, Y. S.; Kucharski, S. A.; Bartlett, R. J. *J. Chem. Phys.* **1984**, *81*, 5906.
- (53) Purvis, G. D.; Bartlett, R. J. *J. Chem. Phys.* **1982**, *76*, 1910.
- (54) Boys, S. F.; Bernardi, F. *Mol. Phys.* **1970**, *19*, 553.
- (55) Bader, R. F. W. <http://www.chemistry.mcmaster.ca/aimpac>, downloaded May 2002.
- (56) Herzberg, G. *Electronic Spectra and Electronic Structure of Polyatomic Molecules*; Van Nostrand: New York, 1966.
- (57) Charo, A.; Delucia, F. C. *J. Mol. Spectrosc.* **1982**, *94*, 426.
- (58) Lubic, K. G.; Amano, T.; Uehara, H.; Kawaguchi, K.; Hirota, E. *J. Chem. Phys.* **1984**, *81*, 4826.
- (59) Alparone, A.; Millefiori, A.; Millefiori, S. *Chem. Phys. Lett.* **2005**, *409*, 288.
- (60) Bak, K. L.; Gauss, J.; Jorgensen, P.; Olsen, J.; Helgaker, T.; Stanton, J. F. *J. Chem. Phys.* **2001**, *114*, 6548.
- (61) Gilli, G.; Bellucci, F.; Ferretti, V.; Bertolasi, V. *J. Am. Chem. Soc.* **1989**, *111*, 1023.